Modeling of Diffraction Effects in Urban Radiowave Propagation

Ozlem Ozgun

Department of Electrical and Electronics Engineering
Hacettepe University, Ankara, 06800, Turkey
ozlem@ee.hacettepe.edu.tr

Abstract ─ A comparative study of some theoretical and numerical models is presented in the solution of two-dimensional urban radiowave propagation problems. The path loss is computed by GO+UTD (geometric optics + uniform theory of diffraction), two-way SSPE (split step parabolic equation) and the diffracting screens models, and the results are compared through numerical simulations. The diffracted fields that are obtained by the GO+UTD model are demonstrated. Computational aspects of the models are briefly discussed.

Index Terms ─ Diffracting screens model, geometric optics (GO), GO+UTD tool, path loss, PETOOL, two-way split step parabolic equation (SSPE), uniform theory of diffraction (UTD), urban propagation.

I. INTRODUCTION

The planning and development of modern mobile communications systems requires accurate and efficient models for urban radiowave propagation, which aim to predict losses in radio signals in different environments. Since the domain of interest is very large in wavelengths, numerical methods like method of moments, finite difference and finite element methods (as well as some commercial software like HFSS, CST, etc.) cannot be employed due to large number of unknowns required to solve such long-range propagation problems. Some empirical models have been developed, which try to estimate propagation losses based on curve-fitting of measured field response [1,2]. However, the main limitation of these models is that they are accurate for specific parameters and environments, and they do not become valid in different propagation scenarios. To overcome the difficulties in empirical models, some theoretical models have been proposed in which the environment is represented by some canonical parameters/geometries, such as building geometry, spacing, etc. For example, Longley-Rice model [3], Bullington model [4], Lee's model [5], and Walfisch and Bertoni model [6,7] have been used in the literature.

There are also some theoretical models, so-called high frequency techniques, such as geometrical optics (GO) [8], geometrical theory of diffraction (GTD) [9], uniform theory of diffraction (UTD) [10], physical optics (PO) [11] and physical theory of diffraction (PTD) [12], which can be used to model urban propagation problems. These techniques use ray-based approach and provide accurate formulations to account for main propagation mechanisms, such as reflection, refraction and diffraction. In Fig. 1, reflection and diffraction of field rays are illustrated in a typical urban propagation problem involving a series of buildings. The GO approach computes incident and reflected fields, but cannot include diffracted fields. Keller extended GO to include diffraction effects and developed GTD by defining a diffraction coefficient for a perfectly conducting wedge by asymptotically evaluating Sommerfelds' diffraction integral. To overcome the singularities along the incident and reflection shadow boundaries (ISB and RSB) in the GTD model, UTD was developed to achieve smoother wave behavior along the shadow boundaries. The PO model estimates the field and current on surface and integrates the current over the surface to determine the scattered field. Similar to GO, the PO does not include the diffracted fields. The PTD method includes the diffracted fields by using non-uniform (fringe) edge currents on the surface. Recently, a MATLAB-based tool (called GO+UTD) was developed to model radiowave propagation by combining the GO and UTD models [13,14]. Also, a MATLAB-based tool for diffraction modeling of a wedge problem was proposed [15,16].

Other than these empirical and theoretical models, parabolic equation (PE) method is perhaps the most efficient numerical method to model arbitrary refraction effects and terrain irregularities in long-range propagation problems [17]. It is based on an approximate form of the Helmholtz wave equation, and can be solved by a marching type algorithm. Therefore, long range propagation problems can easily be solved in a fast and accurate manner. However, one of the limitations of the standard PE is that it considers only forward propagating waves. For short range problems, as well as the problems involving multiple reflections and diffractions because of hills and valleys with steep slopes, the standard PE fails to model multipath effects. To model backward

Submitted On: November 22, 2016
Accepted On: December 26, 2016

propagating waves in an irregular terrain profile, two-way PE model was proposed [18] and implemented as a MATLAB-based tool (called PETOOL) [19]. Although the PE method can inherently model diffracted fields, it cannot separate the diffracted field from the total field.

The organization of this paper is as follows: the GO+UTD, the two-way SSPE and the diffracting screens models are summarized in Sections II, III and IV, respectively. Numerical examples are presented in a comparative manner in Section V. Finally, some conclusions are drawn in Section VI.

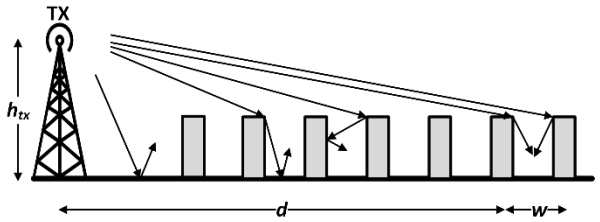

Fig. 1. Radiowave propagation in urban region.

II. GO+UTD MODEL

The GO+UTD toolbox is based on an algorithm that divides the terrain into a number of line segments, and superposes the incident and multiple reflected and diffracted fields by repeatedly utilizing the GO and UTD principles according to different line-of-sight (LOS) conditions [13]. First, direct ray is computed for each illuminated point. Line segments illuminated by the source and their image sources are determined. Reflected rays are computed by radiating these image sources. This process is continued to account for higher-order reflections until the reflected rays escape from the domain, or until the contribution of reflected rays becomes negligible according to a certain threshold criterion. In addition, diffracted fields from sharp tips are computed. The tips behave as new source locations, and the reflected rays of the diffracted rays are computed by obtaining image sources similar to the above steps.

The GO method is illustrated in Fig. 2 (a), where a cylindrically diverging line source is above a flat surface. Assuming that u denotes the electric or magnetic field in horizontal (soft) or vertical (hard) polarizations, respectively, the total field (u^t) in the illuminated part of the surface is the sum of direct/incident field (u^i) and the reflected field (u^r) emanating from the image source, which are given by (assuming $e^{j\omega t}$ time dependence):

$$u^i = u_0 e^{-jkr} / \sqrt{r}\,, \tag{1}$$

$$u^r = u^i\big|_{\text{at } P} R_{s,h} \sqrt{\frac{d_1}{d_1 + d_2}} e^{-jkd_2} = u_0 R_{s,h} \frac{e^{-jk(d_1+d_2)}}{\sqrt{d_1 + d_2}}\,, \tag{2}$$

where u_0 is the amplitude of the incident field, $k = 2\pi/\lambda$ is the wavenumber (λ is the wavelength), and $R_{s,h}$ is the reflection coefficient of the surface, which is -1 and $+1$ for soft and hard polarizations, respectively.

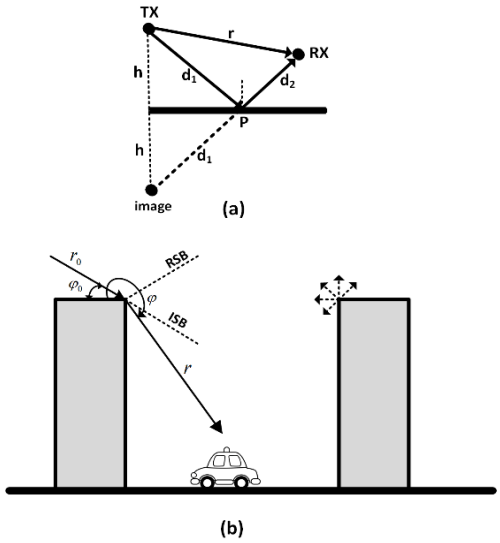

Fig. 2. Illustration of the GO+UTD modeling in the close vicinity of the receiver: (a) GO and (b) UTD.

The UTD method is used to model diffracted fields, and is described by considering the geometry in Fig. 2 (b), which shows the region between two buildings. If the corners of the building are illuminated by either incident field or reflected field from other surfaces, the diffracted fields for each corner are computed and superposed to determine the field at a receiver point. Consider a single corner whose interior wedge angle is $\pi/2$, as shown in the figure. The tip-to-source distance and the source angle are denoted by r_0 and φ_0, respectively; whereas the tip-to-observer distance and the observation angle are represented by r and φ, respectively. The exterior wedge angle is set to $\alpha = 3\pi/2$ to model a right-angled building, and can be set to any value for arbitrary geometries. The diffracted field in UTD is determined by:

$$u^d_{s,h} = u^i D_{s,h}\, \mathrm{e}^{-jkr} / \sqrt{r}\,, \tag{3}$$

where u^i is the incident field at the tip of the wedge, and $D_{s,h}$ is the diffraction coefficient for soft and hard polarizations, given as follows [10]:

$$D_{s,h} = \frac{-e^{-j\pi/4}}{2n\sqrt{2\pi k}} \{ [\cot\left(\frac{\pi - \xi^-}{2n}\right) F(kLg^+\xi^-) + \cot\left(\frac{\pi + \xi^-}{2n}\right) F(kLg^-\xi^-)] \mp [\cot\left(\frac{\pi - \xi^+}{2n}\right) F(kLg^+\xi^+) + \cot\left(\frac{\pi + \xi^+}{2n}\right) F(kLg^-\xi^+)] \}\,, \tag{4}$$

where $(-)$ and $(+)$ are for soft and hard polarizations, respectively. Here, $n = \alpha/\pi, \xi^+ = \varphi + \varphi_0, \xi^- = \varphi - \varphi_0$,

and $F(X)$ is the Fresnel integral given by:

$$F(X) = 2j\sqrt{X}e^{jX}\int_{\sqrt{X}}^{\infty} e^{-j\tau^2}d\tau\,, \tag{5}$$

and L and $g^{\pm}$ are expressed as follows:

$$L = \frac{rr_0}{r+r_0}\,, \quad g^{\pm}(\xi) = 2\cos^2\left(\frac{2n\pi N^{\pm}-\xi}{2}\right), \tag{6}$$

where $N^{\pm} = (\pm\pi+\xi)/2n\pi$ are the integers that most closely satisfy this expression. Since the cotangent functions possess singularities at the shadow boundaries, they can be replaced by (for small $\varepsilon \to 0$):

$$\begin{aligned}&\cot\left(\frac{\pi \pm \beta}{2n}\right)F\left(kLg^{\pm}\xi\right)\\ &\approx n\left[\sqrt{2\pi kL}\,\mathrm{sgn}(\varepsilon) - 2kL\varepsilon e^{-j\pi/4}\right]e^{-j\pi/4}\end{aligned}\,. \tag{7}$$

III. TWO-WAY SSPE MODEL

The parabolic equation (PE) model is widely used in modeling radiowave propagation since electrically long distances can easily be handled by employing a marching-type numerical algorithm. The PE is derived from the Helmholtz wave equation by separating the rapidly varying phase term to get a reduced function varying slowly in range for propagating angles close to the paraxial (horizontal) direction. The PE is converted to an initial value problem and can be solved by the Fourier split-step parabolic equation (SSPE), which starts from an initial field defined by an antenna pattern, and marches in range by determining the field along vertical direction at each range step. The SSPE in its standard form is a one-way approach and accounts for only forward-propagating waves. The field at range $x+\Delta x$ is determined as follows [17-19] (assuming $e^{-i\omega t}$ time dependence):

$$\begin{aligned}&u(x+\Delta x, z) = \exp\left[ik(n-1)\Delta x\right]\times\\ &F^{-1}\left\{\exp\left[ik\Delta x\left(\sqrt{1-\frac{p^2}{k^2}}-1\right)\right]F\left\{u(x,z)\right\}\right\},\end{aligned} \tag{8}$$

where F denotes the Fourier Transform, $p = k_z = k\sin\theta$ is the transform wavenumber where θ is the propagation angle from the horizontal, and n is the refractive index. Equation (8) is known as wide-angle SSPE because it is valid for propagation angles up to 40°-45°.

Since the one-way SSPE model considers only forward propagating waves and ignores backward waves, it cannot model multipath effects accurately if there are some obstacles that re-direct the incoming wave. In [18], a two-way SSPE algorithm was proposed to incorporate the backward waves into the solution, by employing an iterative forward-backward marching algorithm over an irregular terrain. When the wave meets the terrain, it is partially-reflected and is marched out in the opposite direction by reversing the paraxial direction in the PE formulation. This continues until satisfying a stopping criterion that compares the total fields at each iteration. The two-way SSPE algorithm was implemented in MATLAB and named as PETOOL [19].

IV. DIFFRACTING SCREENS MODEL

The diffracting screens model is one of the theoretical models developed by Walfisch and Bertoni [6,7]. In this approach, the rows of city buildings are modeled as a series of absorbing diffracting screens of uniform height. The forward diffraction along the screens, and a final diffraction down to street provides an average field strength at the receiver location (see Fig. 3). This model is polarization independent, and provides a rough estimate about the propagation path loss. In this model, the path loss is obtained by [6,7]:

$$L_{ds} = -L_{fs} - L_1 - L_2 - 18\log\left[\frac{17h_{tx}+d^2}{17h_{tx}}\right], \tag{9}$$

where h_{tx} is the height of the transmitter antenna in meter, and d is the range in km not beyond horizon. Here, F is the free-space propagation loss given by:

$$L_{fs} = 32.4479 + 20\log(fd)\,, \tag{10}$$

where f is the frequency in MHz. The loss L_1 is given as:

$$L_1 = -10\log\left[\frac{G_{rx}(\theta)}{\pi k\sqrt{(h_b-h_{rx})^2+a^2}}\left[\frac{1}{\theta}-\frac{1}{2\pi+\theta}\right]^2\right], \tag{11}$$

where h_b is the height of the building in meter, h_{rx} is the height of the receiver antenna in meter, a is the distance between the building and the receiver in meter, $G_{rx}(\theta)$ is the gain of the receiver antenna along the corner direction, k is the wavenumber, and $\theta = \tan^{-1}((h_b - h_{rx})/a)$ is the angle from the corner to the receiver. The loss L_2 is obtained as:

$$L_2 = -10\log\left[G_{tx}Q^2\right], \tag{12}$$

where G_{tx} is the gain of the transmitter antenna along the corner direction (usually taken as unity), and Q is:

$$Q = \begin{cases}\dfrac{\dfrac{w}{d\times 1000 - w}}{\sqrt{2\pi k\sqrt{(h_b-h_{tx})^2+w^2}}}\left[\dfrac{1}{\theta_1}-\dfrac{1}{2\pi+\theta_1}\right] & \text{if } h_{tx} < h_b - 0.5\sqrt{\lambda w}\\ 2.35\left[\tan^{-1}\left(\dfrac{h_{tx}}{d\times 1000}\right)\sqrt{\dfrac{w}{\lambda}}\right]^{0.9} & \text{if } h_{tx} > h_b + \sqrt{\lambda w}\end{cases}, \tag{13}$$

where w is the distance between buildings in meter, λ is the wavelength, and $\theta_1 = \tan^{-1}((h_b - h_{tx})/w)$.

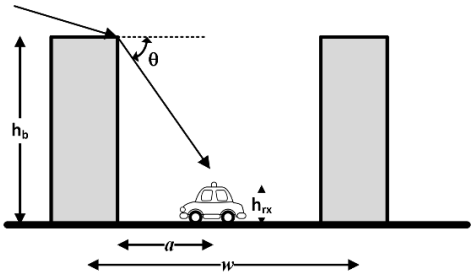

Fig. 3. Illustration of the diffracting screens modeling in the close vicinity of the receiver.

V. NUMERICAL EXAMPLES

This section presents the results of some numerical examples comparing the models in the calculation of path loss. After finding the fields in the SSPE and GO+UTD models, the path loss is obtained by:

$$L = -20\log(u) + 20\log(4\pi) + 10\log\left(a_e \sin\left(x/a_e\right)\right) - 30\log(\lambda), \quad (14)$$

where a_e is the *effective* earth radius to account for the bending of the rays in the standard atmosphere.

In Fig. 4, the 3D maps of path loss obtained by the GO+UTD and two-way SSPE are compared assuming that the frequency is 1800 MHz, the polarization is soft (horizontal), the antenna is omnidirectional and the atmosphere is standard. The range and height step sizes are 0.5 m and 0.2 m, respectively, which are used in other simulations as well. There are 7 buildings, the last of which is $d = 900$ m away from the transmitter at $h_{tx} = 20$ m height. The height of each building is $h_b = 15$ m, and the separation between the buildings is $w = 40$ m. The thickness of each building is 10 m. Due to the height of the transmitter, the field between the buildings is mainly due to the diffracted fields and multiple reflections of the diffracted fields. In Fig. 5, 3D maps of path loss and the magnitude of the diffracted field computed by GO+UTD are plotted for different transmitter heights. The frequency is 900 MHz, and the range is $d = 900$ m. As observed from the results, the field strength between the buildings increases as the transmitter height increases. This is expected due to the contribution of reflected fields at the upper part of the buildings. The behavior of the diffracted field in Fig. 5 (c) is because of the non-physical discontinuities around the incident and reflected shadow boundaries. Dominant diffraction occurs along these critical angles.

In Fig. 6, the path loss is plotted as a function of receiver height for different frequencies, assuming that the receiver is $a = 20$ m away from the buildings. In addition, $d = 600$ m and $h_{tx} = 100$ m. Although the GO+UTD and SSPE models compare well, the results of the diffracting screens model deviate. This is expected because the diffracting screens model does not account for the reflections from the finite thickness of the buildings and the multiple reflections of the diffracted field between the buildings. It is also observed that as the frequency increases, the path loss tends to increase. In Fig. 7, the path loss is plotted as a function of range for different frequencies, assuming that $h_{tx} = 100$ m, $a = 20$ m and $h_{rx} = 1.5$ m. It is seen that as the distance between the buildings and the transmitter antenna increases, the path loss tends to increase. However, due to the interference of diffracted and reflected fields, the path loss may decrease/increase even if the distance increases/decreases. In Fig. 8, the path loss is plotted as a function of receiver height by varying the transmitter height. The frequency is 900 MHz, $d = 900$ m, and $a = 20$ m. As the transmitter height increases, the path loss tends to decrease between the buildings. Finally, in Fig. 9, the GO+UTD and two-way SSPE models are compared for arbitrarily-shaped and positioned buildings. Note that the diffracting screens model is not applicable in this configuration.

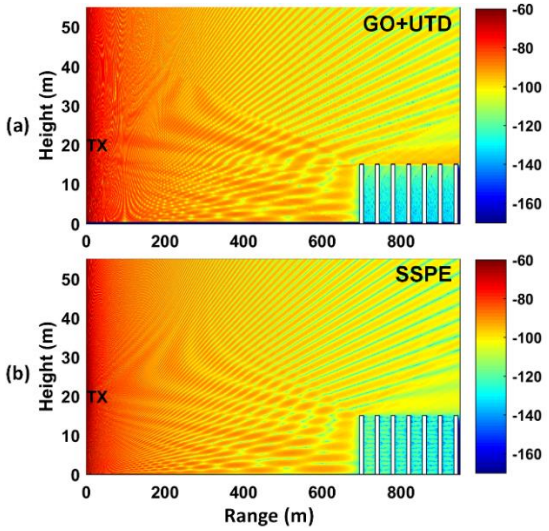

Fig. 4. 3D maps of path loss in 1800 MHz: (a) GO+UTD, and (b) two-way SSPE.

When the computational performances of the models are compared, it is evident that the diffracting screens model quickly performs in a few seconds, but its accuracy is less. Although the SSPE and GO+UTD models involve heavier computational load, they provide accurate results. The computation time of the SSPE and GO+UTD models depend on many factors, such as the distance, the level of discretization in the domain (range and height step sizes), the level of accuracy (the difference in the field distribution when each contributing field is added) and especially the interaction between the radiated fields and the buildings. Depending on the location of the antenna and the buildings, the amount of wave interactions (multiple reflections and diffractions) determine the amount of calculations and the computation

time. The GO+UTD tool has been parallelized in MATLAB by using the parallel processing tools to perform the computations in parallel for each point within the LOS of each source. Hence, the performance of the GO+UTD also depends on the number of processors used. The two-way SSPE performs sequential computations, but this tool will be parallelized in the near future. The 3D maps of the example in Fig. 9 were obtained by GO+UTD in 27mins with 4 processors, and by SSPE in 20mins (12mins) for 1500 (1000) number of step-wise forward-backward calculations. Note that the discretization is taken quite fine (256×380 grid) to obtain better looking maps. The time will decrease if less receiver points are needed in the domain.

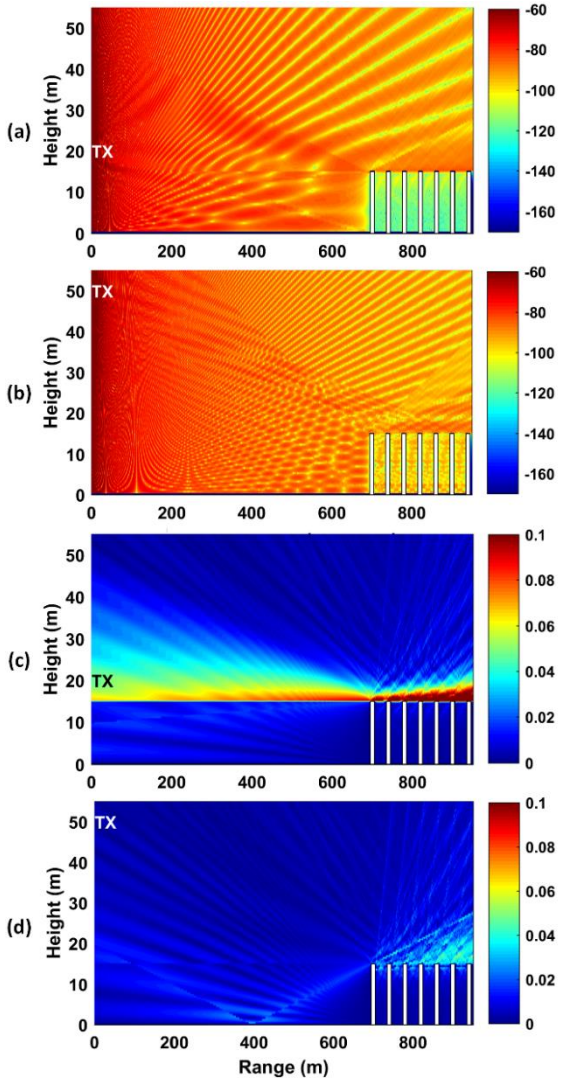

Fig. 5. 3D maps of path loss and the magnitude of the diffracted field computed by GO+UTD in 900 MHz: (a) path loss with $h_{tx} = 20$ m, (b) path loss with $h_{tx} = 50$ m, (c) diffracted field with $h_{tx} = 20$ m, and (d) diffracted field with $h_{tx} = 50$ m.

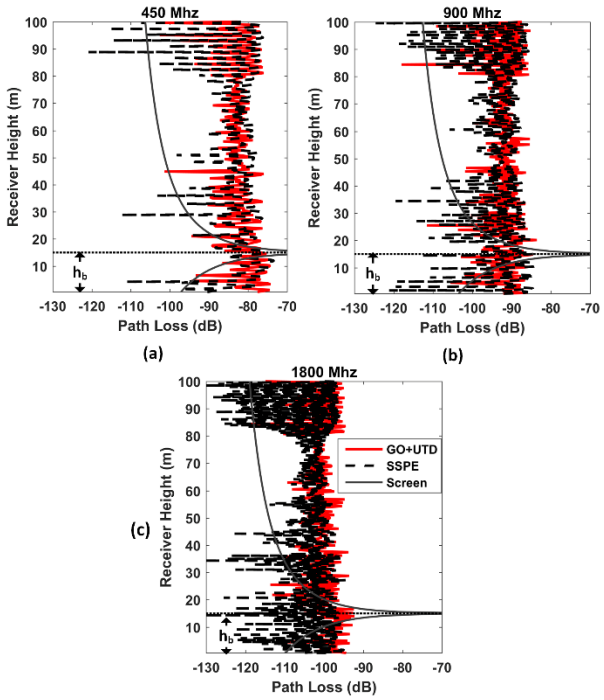

Fig. 6. Path loss as a function of receiver height: (a) 450 MHz, (b) 900 MHz, (c) 1800 MHz. ($d = 600$ m, $h_{tx} = 100$ m, $a = 20$ m).

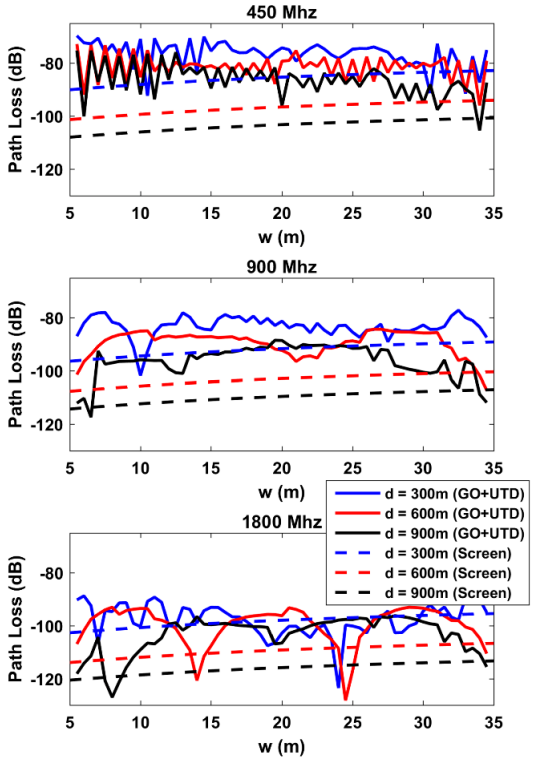

Fig. 7. Path loss as a function of range: (a) 450 MHz, (b) 900 MHz, (c) 1800 MHz. ($h_{tx} = 100$ m, $a = 20$ m, $h_{rx} = 1.5$ m).

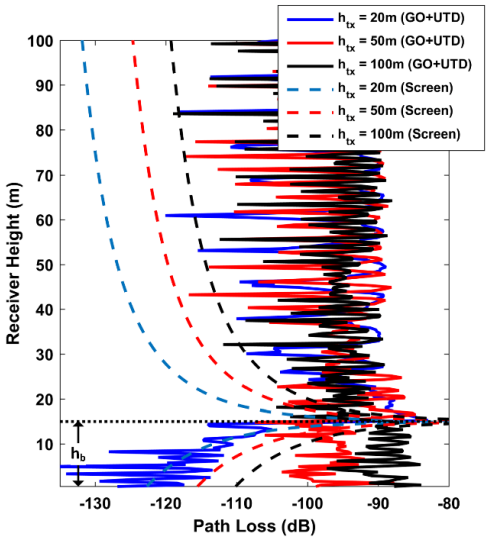

Fig. 8. Path loss as a function of receiver height for different transmitter heights. ($f = 900$ MHz, $d = 900$ m, $a = 20$ m).

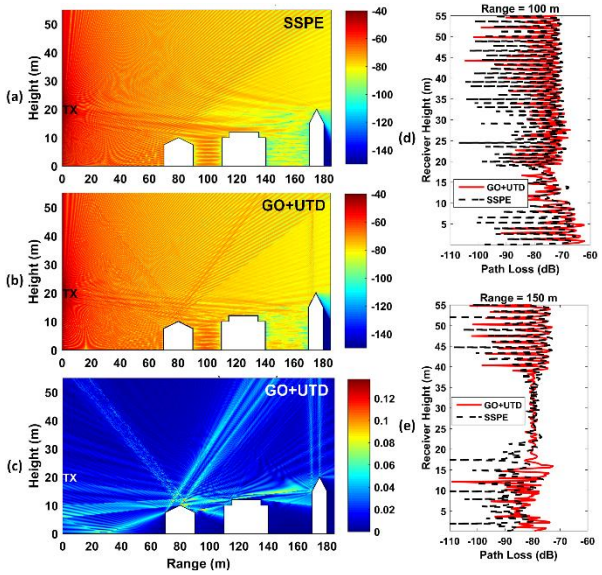

Fig. 9. Simulation of arbitrarily-shaped and -positioned buildings at 900 MHz: (a) path loss (two-way SSPE), (b) path loss (GO+UTD), (c) diffracted field (GO+UTD), (d) path loss vs. receiver height (at 100 m range), and (e) path loss vs. receiver height (at 150 m range).

VI. CONCLUSION

Three models (GO+UTD, two-way SSPE and the diffracting screens models) have been considered for the solution of radiowave propagation in urban area. It is observed that the diffracting screens model provides a rough estimate for the path loss and is not capable of modeling interference effects due to multiple reflections and diffractions. However, the SSPE and GO+UTD provide accurate results, and the GO+UTD model is useful to visualize the diffracted fields. The GO+UTD and the two-way SSPE compare well in general, except for small differences around the shadow boundaries and in the deep shadow region, which can be improved by decreasing the step size.

REFERENCES

[1] Y. Okumura, E. Ohmori, T. Kawano, and K. Fukua, "Field strength and its variability in UHF and VHF land-mobile radio service," *Rev. Elec. Commun. Lab.*, vol. 16, no. 9, 1968.

[2] M. Hata, "Empirical formula for propagation loss in land mobile radio services," *IEEE Trans. Veh. Technol.*, vol. VT-29, no. 3, pp. 317-325, 1980.

[3] A. G. Longley and P. L. Rice, "Prediction of tropospheric radio transmission loss over irregular terrain—A computer method," *ESSA Technical Report ERL*, 79-IOTS 67, 1968.

[4] K. Bullington, "Radio propagation for vehicular communications," *IEEE Transactions on Vehicular Technology*, vol. VT-26, no. 4, pp. 295-308, 1977.

[5] W. C. Y. Lee, *Mobile Communications Engineering*. McGraw-Hill, New York, 1982.

[6] J. Walfisch and H. L. Bertoni, "A theoretical model of UHF propagation in urban environments," *IEEE Transactions on Antennas and Propagation*, vol. 36, pp. 1788-1796, 1988.

[7] K. Siwiak, *Radiowave Propagation and Antennas for Personal Communications*. Artech House, 2007.

[8] M. Kline and I. Kay, *Electromagnetic Theory and Geometrical Optics*. Wiley, New York, 1965.

[9] J. B. Keller, "Geometrical theory of diffraction," *J. Opt. Soc. Amer.*, vol. 52, pp. 116-30, 1962.

[10] R. G. Kouyoumjian and P. H. Pathak, "A uniform geometrical theory of diffraction for an edge in a perfectly conducting surface," *Proc. IEEE*, vol. 62, pp. 1448-1461, 1974.

[11] A. K. Bhattacharyya, *High Frequency Electromagnetic Techniques Recent Advances and Applications*. Wiley, 1995.

[12] P. Y. Ufimtsev, *Theory of Edge Diffraction in Electromagnetics* Tech Science Press, 2003.

[13] O. Ozgun, "New software tool GO+UTD for visualization of wave propagation," *IEEE Antennas Propag. Mag.*, vol. 58, pp. 91-103, 2016.

[14] O. Ozgun and L. Sevgi, "Numerical techniques in modeling electromagnetic scattering from single and double knife-edge in 2D ground wave propagation problems," *ACES, Appl. Comput. Electrom.*, vol. 27, no. 5, pp. 376-388, 2012.

[15] F. Hacivelioglu, M. A. Uslu, and L. Sevgi, "A MATLAB-based virtual tool for the electromagnetic wave scattering from a perfectly reflecting wedge," *IEEE Antennas Propag. Mag.*, vol. 53, pp. 234-243, 2011.

[16] G. Apaydin and L. Sevgi, "Penetrable wedge scattering problem and a MATLAB-based fringe wave calculator," *IEEE Antennas Propag. Mag.*, vol. 58, pp. 86-93, 2016.
[17] M. F. Levy, *Parabolic Equation Methods for Electromagnetic Wave Propagation*, *IEEE Electromagnetic Wave Series*, London, 2000.
[18] O. Ozgun, "Recursive two-way parabolic equation approach for modeling terrain effects in tropospheric propagation," *IEEE T Antenn. Propag.*, vol. 57, no. 9, pp. 2706-2714, 2009.
[19] O. Ozgun, G. Apaydin, M. Kuzuoglu, and L. Sevgi, "PETOOL: MATLAB-based one-way and two-way split-step parabolic equation tool for radiowave propagation over variable terrain," *Comput. Phys. Commun.*, vol. 182, no. 12, pp. 2638-2654, 2011.